

A 65nm CMOS Ultra Low Power and Low Noise 131M Ω Front-End Transimpedance Amplifier

Jiaping Hu

Department of Electrical and
Computer Engineering
Northeastern University
Boston, Massachusetts
jhu@ece.neu.edu

Yong-Bin Kim

Department of Electrical and
Computer Engineering
Northeastern University
Boston, Massachusetts
ybk@ece.neu.edu

Joseph Ayers

Department of Biology and
Marine Science Center
Northeastern University
Nahant, Massachusetts
lobster@neu.edu

ABSTRACT

In this paper, the design, implementation and simulation of a high-transimpedance gain, ultra low-power dissipation and low-noise CMOS front-end transimpedance amplifier (TIA) is presented. For interfacing with bio-sensor array and analog neuron circuit, an improved capacitive-feedback TIA topology is adopted with active load to obtain a 131M Ω gain, 1.45MHz bandwidth, 90.8fA/rt(Hz) input-referred current noise at the sampling frequency, less than 1 $^\circ$ phase response at the sampling frequency, and 520mV peak-to-peak output swing. The proposed circuit dissipates less than 30 μ W with 0.8V supply voltage, and the circuit is implemented in 65nm CMOS Predictive Technology Model.

I. INTRODUCTION

Recent advances in biomimetics, such as electronic nervous systems (ENS) based on nonlinear dynamical models of neurons and synapses have made it feasible to control robots using biological control mechanisms [1]. Due to the stringent power, supply, area and robustness requirements in such applications, an integrated circuit approach becomes essential. Without the need for data converters and FSM, analog electronic implementations, as shown in Fig. 1, provide the desired ability of continuous-time and adaptive control [3]. However, it introduces design challenges in the form of trade-offs between noise, power dissipation, speed, and process variations.

A biohybrid underwater robot 'Cyberplasm' with an analog electronic nervous system is shown in Fig.2. A primary problem is the interface between cellular reporters and electronic neurons. The amplitude of the current signal is constrained to the

level of nanoamps [4] due to low-power operation, limited sensing ability, and low quantum efficiency of silicon. Moreover, since the TIA works as a preamplifier of the level-sensitive analog neuron circuit, a high output swing is also desired. Nevertheless, although the sensing frequency of the biosensor arrays in our system is limited to 5KHz, the frequency response of the TIA should be well beyond the bio-oscillation frequency of CPG in order to reduce its phase noise [6]. In this paper, we present a novel front-end TIA design that provides a high gain, low input-referred current noise, high output swing, and proper frequency /phase response in a 65nm CMOS process.

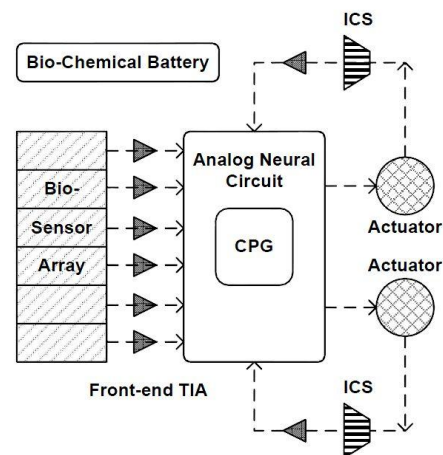


Figure 1: Block diagram of a biohybrid robot consists of front-end biosensor array, analog neural circuit with CPG, actuators followed by synthetic muscle, intersegment coordinating systems(ICS), transimpedance amplifier in the optical-signal path (dash lines), and bio-chemical fuel cell.

The paper is organized as follows. Section II introduces and analyzes the topology used in the design. Simulation results are presented in Section III followed by Section IV, where the performance of the TIA and a comparison with prior arts are summarized.

This project was supported by the US National Science Foundation under the Grant CBET-0943345.

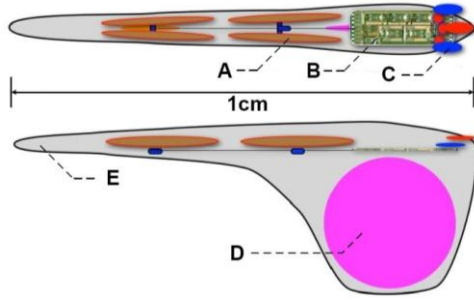


Figure 2: Sea Lamprey-based Biohybrid Robot 'Cyberplasm' [1]. A: Synthetic muscle; B: Electronic nervous system; C: Bio-sensor array; D: Fuel cell; E: Hydrogel/Polymer backbone

II. CIRCUIT IMPLEMENTATION

A. Improved Capacitive-Feedback TIA

The most commonly used topology of a TIA applies a resistive-feedback mechanism, as shown in Fig.3(a). The feedback resistor R_F with a parallel C_F (not shown in the figure) sets the gain and frequency response. Another popular topology harnesses a capacitive feedback loop only, which eliminates the noise contribution from R_F . The improved TIA topology used in our low noise, high gain biosensor application is shown in Fig.3(c). First demonstrated in [5], it exhibits several advantages for our continuous biohybrid robot control application over the commonly used resistive method shown in Fig.3(a) or capacitive-feedback TIAs shown in Fig.3(b).

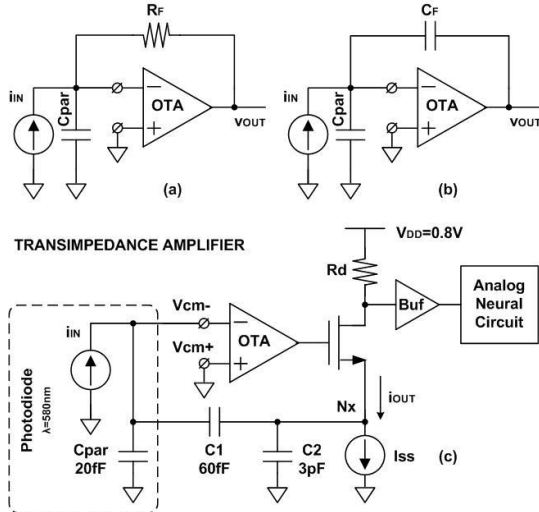


Figure 3: (a) Resistive feedback TIA; (b) Capacitive feedback TIA; (c) The schematic of the proposed TIA design with the improved capacitive feedback single-ended topology

First, the capacitive-feedback current amplifier in Fig.3(c) drives current to the high impedance

output with a gain of $(1+C_2/C_1)$. Meanwhile, the resulting large transimpedance gain of $(1+C_2/C_1) \cdot R_d$, which in turn, reduces the input-referred current noise due to the load R_d by the same factor [5,6] as shown in (2), where ω is frequency, k is the Boltzmann constant, T is temperature and v_N^2 is the amplifier input-referred voltage noise. Comparing with the resistive-feedback TIA, the proposed topology alleviates the trade-off between noise and gain.

Second, comparing with the common capacitive-feedback TIAs shown in Fig.3(b), the OTA in the feedback loop adds an additional 180° phase shift to the improved topology in Fig.3(c), thus avoiding the nonzero phase-response seen in Fig.3(b). It also pushes the location of the pole from large C_2 away by a factor of $(1+A_0)$ as shown in (3) [5], where g_{m2} is the transconductance of transistor M_2 and A_0 is the DC gain of the OTA. The equation also implies the possibility of increasing bandwidth by increasing the gain of the OTA in the new topology without reducing R_d and the transimpedance gain.

$$Gain = R_D \cdot \left(1 + \frac{C_2}{C_1}\right) \quad (1)$$

$$i_N^2 = \frac{4kT}{R_D(1+\frac{C_2}{C_1})^2} + v_N^2 \omega^2 (C_1 + C_{par})^2 \quad (2)$$

$$BW_{TIA} = \frac{g_{m2}(1+A_0)C_1}{C_2(C_1+C_{par})} \quad (3)$$

As a result, the adopted topology relaxes the trade-offs between gain, noise and bandwidth in the desired transimpedance amplifier design. However, the noise and bandwidth of this improved capacitive feedback topology will be affected by the parasitic of the photodiode, as shown in (2), (3).

For further power reduction, transistors in the proposed TIA operate in the weak inversion region. The load of the TIA is implemented with a long-channel PMOS transistor for maximizing the transimpedance gain. Finally, the active load is sized to $12.9\mu\text{m}/0.3\mu\text{m}$ to balance among the gain, bandwidth and noise performance.

B. Miller Two-Stage OPAMP

As discussed in the previous sections, a Miller Two-Stage OPAMP with high gain, suitable GBW, and low-power is designed for the capacitive feedback loop of the proposed TIA. The circuit schematic of the proposed Miller 2-stage OPAMP is shown in Figure 4. Weak-inversion operation is

adopted for the transistors of the OPAMP because of the low-power and low voltage operation requirements.

Transistors in the current mirror throughout the OPAMP are biased with large V_{GS} to minimize the mismatch and noise [7]. Table I summarized the OPAMP's simulated characteristics. Figure 5 shows the schematic of its constant-gm bias circuit of the design [5].

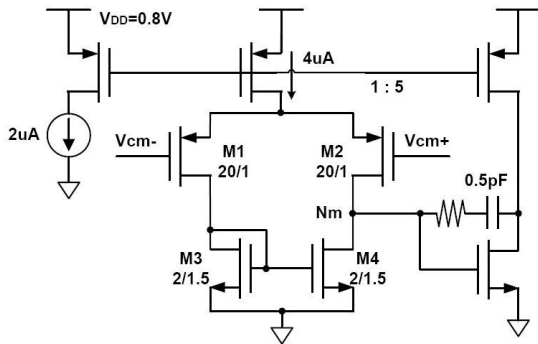


Figure 4: Schematic of the proposed miller two-stage OPAMP

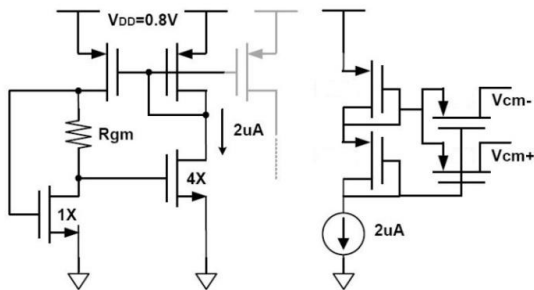


Figure 5: Schematic of the constant-gm bias circuit and input common-mode bias circuit

Table I: Summary of the Simulated Opamp Performance

Parameter	Measured Value
Technology	65nm CMOS
Power Supply	0.8V
DC Gain	85dB
Unity GBW	11MHz w/ 2pF load
Phase Margin	70.8°
Noise Floor	38.6nV/rt(Hz)
Power Dissipation	19.6μW

III. SIMULATION RESULTS

Simulation results of AC analysis are shown in Fig.6. The proposed TIA exhibits a 131MΩ transimpedance gain, which not only ensures the

correct functionality of the level-sensitive analog neural circuit, but also relaxes the noise requirement of the system. Meanwhile, it keeps a flat frequency-response up to 1.45MHz, which is more than adequate for controlling the underwater robot. Moreover, the TIA shows a phase-response within 10° from 4Hz to 165KHz, thus the in-phase control of the system is achieved. Input-referred current noise, as shown in Fig.7, is controlled under 91fA/rt(Hz) at 5KHz. Thus the desired low-noise performance of the front-end TIA is achieved.

The transient performance is also measured at the practical operating frequency of the electronic CPG. The TIA exhibits a 520mV peak-to-peak output voltage swing as shown in Fig.8. The in-phase signal amplification of the circuit is also observed from this transient analysis.

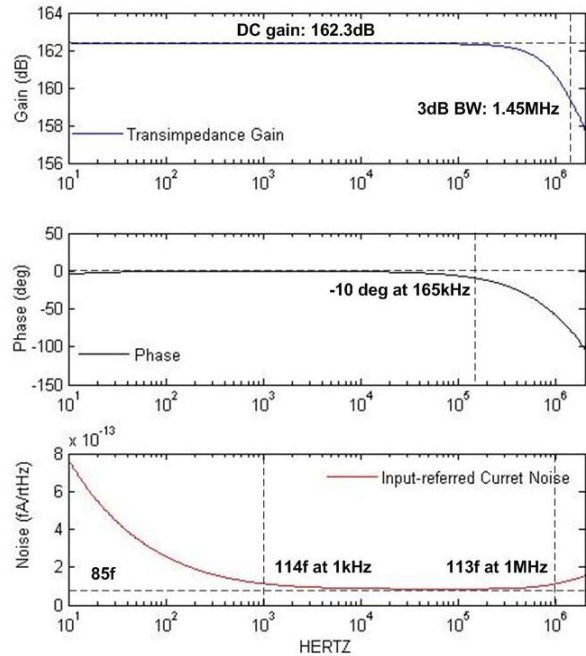


Figure 6: Transimpedance gain, phase response and noise

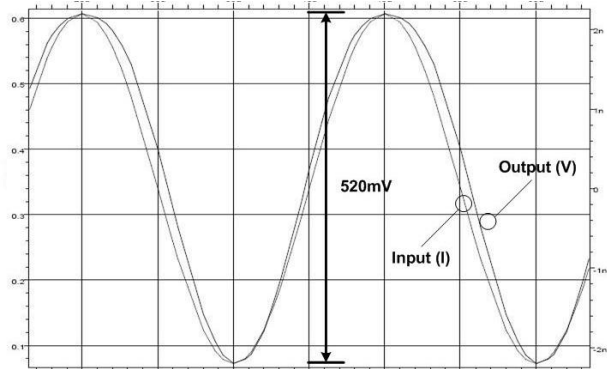


Figure 7: Maximum output voltage swing of the TIA. Left Y-Axis: Output voltage; Right Y-Axis: Input current

Table II: Power Dissipation of the TIA

Block	Power
OPAMP	19.6 μ W
Constant-gm Bias	4.4 μ W
Output stage	4 μ W
Total	29.3 μ W

IV. SUMMARY

The proposed design achieves 131M Ω transimpedance gain, 1.45MHz 3dB-Bandwidth and less than 7 $^\circ$ phase shift between 5KHz-100KHz. With an additional flexibility in design trade-offs between gain and bandwidth, the AC performance of the proposed TIA is suitable for biosensing applications. Low current consumption (37 μ A) as well as low input-referred current noise (90.8A/rt(Hz)) are obtained in the design. Finally, a 520mV peak-to-peak output voltage swing is measured. That allows its application in biohybrid robot control systems.

The power dissipation of the TIA is measured and summarized in Table II. Table III shows a comparison with prior arts. The topology of the proposed design was first demonstrated in [5]. TIA in the second column was designed for MEMS applications, which have a very similar set of design specifications as biosensing applications in the last three columns.

IV. CONCLUSION

This paper describes a transimpedance amplifier for cellular biosensors. It utilizes an improved capacitive-feedback topology to avoid the design issue from large on-chip resistors and to increase the design flexibility in gain-bandwidth

trade-off. The proposed TIA is implemented in PTM 65nm technology. The design demonstrates a 131M Ω transimpedance gain with 1.45MHz BW, less than 7 $^\circ$ phase response between 5KHz-100KHz, 520mV Peak-to-Peak voltage swing, 90.8fA/rt(Hz) input-referred current noise, while dissipating 30 μ W power with 0.8V power supply.

REFERENCES

1. Ayers, J. and N. Rulkov (2007). Controlling Biomimetic Underwater Robots with Electronic Nervous Systems. In: Bio-mechanisms of Animals in Swimming and Flying. N. Kato and S. Kamimura. Tokyo, Springer-Verlag. Pp. 295-306.
2. Shuenn-Yuh Lee; Chih-Jen Cheng; Cheng-Pin Wang; Shyh-Chyang Lee. "A 1V 8Bit 0.95mW Successive Approximation ADC for Biosignal Acquisition Systems", ISCAS 2009. IEEE.
3. J. Lee, Y. J. Lee, K. Kim, Y. B. Kim, and J. Ayers (2007) "Low Power CMOS Adaptive Electronic Central Pattern Generator Design for a Biomimetic Robot", Neurocomputing 71: 284-296.
4. Indal Song, "Multi-Gbit/s CMOS Transimpedance Amplifier with Integrated Photodetector for Optical Interconnects", PhD Thesis.
5. B. Razavi, "A 622Mb/s 4.5pA/ \sqrt Hz CMOS transimpedance amplifier", ISSCC Tech. Digest, San Francisco, CA, Feb. 7-9, 2000, pp. 162-163.
6. James Salvia, Pedram Lajevardi, Mohammad Hekmat, and Boris Murmann, "A 56M Ω CMOS TIA for MEMS Applications", CICC 2009.
7. P.R.Gray, R.G.Meyer, P.J.Hurst, and S.H.Lewis, <Analysis and Design of Analog Integrated Circuits> .Hoboken,NJ: Wiley,2001.
8. Jiaping Hu, Yong-Bin Kim, "A Low Power 100M Ohm CMOS Front-End Transimpedance Amplifier for Biosensing Applications", 2010 Midwest Symposium on Circuits and Systems, Seattle, WA.(Submitted).
9. G. Ferrari, F. Gozzini, M. Sampietro, "A current-sensitive front-end amplifier for nano-biosensors with a 2MHz BW", ISSCC Dig. Tech. Papers, pp. 164-165, Feb. 2007.

Table III. Comparison with Prior Arts

Parameter	[5]	[6]	[9]	[8]	This work
Application	Receiver	MEMS	Biosensor	Biosensor	Biosensor
Technology	0.6 μ m CMOS	0.18 μ m CMOS	0.35 μ m CMOS	0.18 μ m CMOS	65nm CMOS
Supply	3V	1.8V	3.3V	1.8V	0.8V
DC Gain	8.7k Ω	56M Ω	30M Ω	100M Ω	131M Ω
Bandwidth	550MHz	1.8 MHz	2 MHz	1 MHz	1.45 MHz
Input noise	4.5pA/rtHz	65fA/rtHz	3fA/rtHz	134fA/rtHz	90.8fA/rtHz
Power	30mW	436 μ W	21mW	132 μ W	29.3 μ W